Inorganic Chemistry

Article

pubs.acs.org/IC

Monoammoniate of Calcium Amidoborane: Synthesis, Structure, and Hydrogen-Storage Properties

Yong Shen Chua,[†,‡] Hui Wu,*[,§,∥] Wei Zhou,[§,∥] Terrence J. Udovic,[§] Guotao Wu,*[,†] Zhitao Xiong,[†] Ming Wah Wong,[‡] and Ping Chen[†]

[†]Dalian Institute of Chemical Physics, Dalian 116023, People's Republic of China.

[‡]Department of Chemistry, National University of Singapore, Singapore 117542, Singapore

[§]NIST Center for Neutron Research, National Institute of Standards and Technology, Gaithersburg, Maryland 20899-6102, United States

[∥]Department of Materials Science and Engineering, University of Maryland, College Park, Maryland 20742-2115, United States

Supporting Information

ABSTRACT: The monoammoniate of calcium amidoborane, $Ca(NH_2BH_3)_2{\cdot}NH_3$, was synthesized by ball milling an equimolar mixture of CaNH and AB. Its crystal structure has been determined and was found to contain a dihydrogen-bonded network. Thermal decomposition under an open-system begins with the evolution of about 1 equivalent/formula unit (equiv.) of NH_3 at temperatures <100 °C followed by the decomposition of $Ca(NH_2BH_3)_2$ to release hydrogen. In a closed-system thermal decomposition process, hydrogen is liberated in two stages, at about 70 and 180 °C, with the first stage corresponding to an exothermic process. It has been found that the presence of the coordinated NH_3 has induced the dehydrogenation to occur at low temperature. At the end of the dehydrogenation, about 6 equiv. (∼ 10.2 wt %) of hydrogen can be released, giving rise to the formation of CaB_2N_3H.

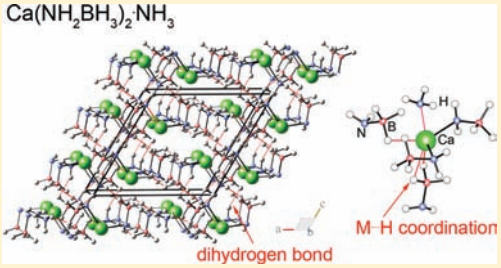

INTRODUCTION

The increasing scarcity of fossil fuels and their link to global warming underscores the need to shift our current energy sources to more environmentally friendly and efficient alternatives. Hydrogen has been regarded as the most promising future fuel as it is high in energy and when it burns, it produces no pollution. However, one of the most important technological challenges facing a hydrogen economy is the development of safe and energy-efficient hydrogen-storage materials, especially for use with hydrogen fuel-cell vehicles. Ammonia borane (NH_3BH_3, AB) has drawn significant attention as one of the potential hydrogen-storage materials because of its high hydrogen capacity (ca. 19.6 wt %) and moderate dehydrogenation properties. However, its widespread application is restricted because of the slow dehydrogenation kinetics and the release of volatile by-product.[1,2] Aiming to improve its hydrogen storage properties, active research activities have been focused on the catalytic dehydrocoupling of ammonia borane and its derivatives, that is, primary and secondary amineboranes (RNH_2BH_3 and R_2NHBH_3).[3−6] Besides kinetic improvement, ammonia borane with its potential N−H group which protonic H^+ is of the weak Lewis acidity, could be functionalized for thermodynamic improvement. As results of the introduction of a functional group by reacting ammonia borane with a stronger Lewis acid, that is, metal hydrides, a series of single-metal and double-metal amidoboranes consisting of metal cations and amidoborane anions were developed, including amidoboranes of Li,[7,8] Na,[7] K,[9] Ca,[10,11] Sr,[12] Y,[13] Na_2Mg,[14] NaMg,[15] and NaLi.[16] These metal amidoboranes are found to exhibit significant improvement over the parent AB, including reduced dehydrogenation temperature with moderate dehydrogenation thermodynamics, improved dehydrogenation kinetics, and suppression of the release of volatile byproduct. In addition, intensive mechanistic investigations were also studied to understand the role of metal cation in the improved dehydrogenation properties.[3,17−21]

Besides metal hydrides, metal amides or imides, which typically contain strong Lewis bases NH_2^- or NH^{2-}, would likewise undergo acid−base reactions with AB. As a result, several new hydrogen-storage materials, ammoniates of amidoborane, were synthesized, such as $Ca(NH_2BH_3)_2{\cdot}2NH_3$,[22] $Mg(NH_2BH_3)_2{\cdot}NH_3$,[23] $LiNH_2BH_3{\cdot}NH_3$.[24,25] These ammoniates demonstrated significantly improved dehydrogenation properties owing to the active participation of NH_3 in the dehydrogenation process. Despite the salient role of NH_3 in the ammoniate complexes, contamination of H_2 by a small amount of NH_3 is unavoidable. It is worth mentioning that the presence of even a few ppm of NH_3 would poison the fuel cell. Earlier study in the investigation of the ammoniate samples revealed that by reducing the amount of N−H group in the starting materials,

Received: August 30, 2011
Published: January 9, 2012

   dx.doi.org/10.1021/ic201898v | *Inorg. Chem.* 2012, 51, 1599−1603

that is, using MgNH instead of $Mg(NH_2)_2$, monoammoniate of magnesium amidoborane can be formed, and it demonstrates the capability of complete conversion of NH_3 to H_2 in the dehydrogenation process.[23] Therefore, in this study, we tentatively reduced the NH_3 content in the diammoniate of calcium amidoborane and demonstrated that by employing a calcium imide modification on ammonia borane, a new ammoniate compound, namely, calcium amidoborane monoammoniate, $Ca(NH_2BH_3)_2{\cdot}NH_3$, can be synthesized with less NH_3 contamination in the gaseous product during its decomposition in a closed-system.

EXPERIMENTAL SECTION

Materials and Handlings. NH_3BH_3 and CaH_2 powder were purchased from Sigma Aldrich and Fluka with claimed purity of 97% and >97%, respectively. $Ca(NH_2)_2$ and CaNH were synthesized as described in refs 22 and 26, respectively.[27] A mixture of CaNH and NH_3BH_3 in a 1:2 molar ratio was ball milled under an inert atmosphere for 10 h on a Retsch PM400 planetary mill. Ball milling gave a solid product and hardly any gaseous product could be detected. A mixture of $Ca(NH_2)_2$, CaH_2, and AB with the molar ratio of 1:1:4 was also ball milled and approximately 2 equiv. moles of H_2 was released. All the materials handlings were performed in a glovebox filled with argon gas.

Characterization. Qualitative investigation of gaseous products formed during the dehydrogenation was performed on a custom-made temperature-programmed desorption/mass spectrometry (TPD-MS) apparatus. Thermal analyses were conducted on a Netzch 449C TG/DSC (thermogravimetry-differential scanning calorimetry) unit. In the TPD-MS and TG-DSC experiments, purified argon was used as carrier gas in a dynamic flow mode with a heating rate of 2 °C/min. Volumetric release was carried out on a custom-made reactor. Gas-phase ammonia concentration was quantified by using a Thermo conductivity meter where the accumulated gaseous product (formed during volumetric release measurement) was bubbled into a dilute H_2O solution and the change in ion conductivity of the solution was monitored. Structural identifications were carried out on a PAnalytical X'pert diffractometer with Cu Kα, 40 kV, 40 mA, and the synchrotron X-ray powder diffractometer at the Shanghai Synchrotron Radiation Facility. Solid state ^{11}B MAS NMR experiments were carried out on a DRX400 spectrometer (9.4T) at ambient temperature. FTIR measurements were conducted on a Varian 3100 unit in DRIFT mode. Raman spectra were recorded on a commercial micro-Raman spectrometer (Renishaw) equipped with a CCD detector, using a He/Ne laser with a wavelength of λ = 514 nm. Neutron vibrational spectra (NVS) were measured at 5 K using the BT-4 Filter-Analyzer Neutron Spectrometer (FANS) at NIST with the Cu(220) monochromator under conditions that provided energy resolutions of 2−4.5% over the vibrational energy range probed.

RESULTS AND DISCUSSION

An X-ray diffraction (XRD) pattern was collected on the postmilled mixture of CaNH + 2AB and is shown in Figure 1. A new phase was obtained which does not match any known compound found in the database, indicating a complete conversion of the starting materials to the new phase. ^{11}B MAS NMR characterization (Figure 2) revealed the presence of a single boron resonance at about −21 ppm in the postmilled sample, which is similar to the chemical shift found for the $Ca(NH_2BH_3)_2{\cdot}2NH_3$,[22] indicating the formation of a new single boron species with identical boron environment. The FTIR and Raman spectra (see Supporting Information, Figure S1 and S2) of $Ca(NH_2BH_3)_2{\cdot}NH_3$ revealed several distinct bands in the N−H stretching (3000−3400 cm^{-1}) and B−H stretching (2000−2500 cm^{-1}) regions. The N−H stretching of $Ca(NH_2BH_3)_2{\cdot}NH_3$ (Raman spectra) displays five sharp

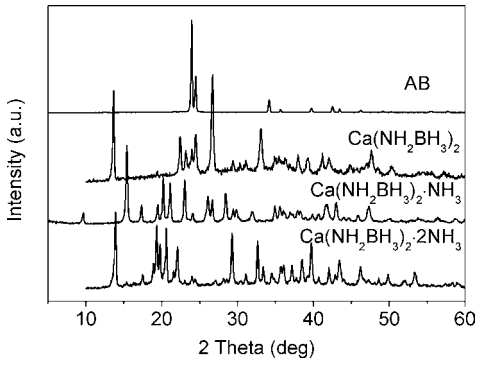

Figure 1. Comparison of the XRD patterns for the $Ca(NH_2BH_3)_2{\cdot}NH_3$ (CaNH/2AB), $Ca(NH_2BH_3)_2{\cdot}2NH_3$ ($Ca(NH_2)_2$/2AB), $Ca(NH_2BH_3)_2$, and pristine AB.

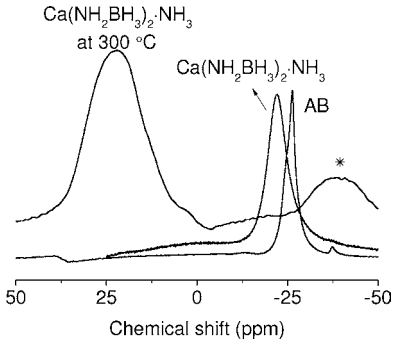

Figure 2. Comparison of the ^{11}B MAS NMR spectra of pristine AB, $Ca(NH_2BH_3)_2{\cdot}NH_3$ (CaNH/2AB), and the postdehydrogenated sample and pristine AB. The asterisk denotes the spinning sideband.

distinct peaks (3278, 3310, 3322, 3368, and 3380 cm^{-1}) which appear in the same region with those of $Ca(NH_2BH_3)_2{\cdot}2NH_3$. Furthermore, the B−H stretching modes in both samples are indistinguishable. Hence, the similarities point to similar N−H and B−H species in both structures. However, in comparison to the B−N, N−H, and B−H stretching modes detected in AB, a substantial blue shift of B−N and N−H stretching and a red shift of B−H stretching were detected, revealing a substantial change in the bond strength after CaNH modification of AB. The results described above suggest that eq 1 has occurred because of reaction of CaNH with AB in the ball-milling process:

$$CaNH + 2NH_3BH_3 \rightarrow Ca(NH_2BH_3)_2{\cdot}NH_3 \quad (1)$$

From the chemical composition point of view, $Ca(NH_2BH_3)_2{\cdot}NH_3$ may be synthesized by reacting $Ca(NH_2BH_3)_2{\cdot}2NH_3$ and $Ca(NH_2BH_3)_2$. To prove this hypothesis, we tentatively ball milled $Ca(NH_2)_2$, CaH_2, and AB with the molar ratio of 1:1:4. At the end of ball milling, about 0.5 equiv. of H_2 per AB were detached. Inspection on its XRD pattern reveals an identical set of diffraction peaks with that of postmilled CaNH-2AB (see Supporting Information, Figure S3), indicating the formation of $Ca(NH_2BH_3)_2{\cdot}NH_3$ as described in eq 2.

$$Ca(NH_2)_2 + CaH_2 + 4AB \rightarrow Ca(NH_2BH_3)_2{\cdot}NH_3 + 2H_2 \quad (2)$$

As earlier proposed in the formation of $Ca(NH_2BH_3)_2{\cdot}2NH_3$ that there are two possible reaction mechanisms, the strong

dx.doi.org/10.1021/ic201898v | Inorg. Chem. 2012, 51, 1599−1603

base of amide (NH_2^-) may either abstract an H^+ or a BH_3 of NH_3BH_3 to form NH_3 and a $NH_2BH_3^-$ anion.[22] In the interaction of CaNH and AB, $Ca(NH_2BH_3)_2{\cdot}NH_3$ was formed instead of $Ca(NHBH_3)_2{\cdot}2NH_3$. Therefore, it is likely that the strong Lewis base $(NH)^{2-}$ would abstract an H^+ from each AB, leading to the formation of NH_3 and amidoborane anion $NH_2BH_3^-$.

On the basis of the XRD data, the crystal structure of the postmilled sample was determined to be $Ca(NH_2BH_3)_2{\cdot}NH_3$, the monoammoniate of calcium amidoborane, which crystallizes in a monoclinic cell with the space group of $P2_1/c$ and the lattice parameters of a = 10.5831(14) Å, b = 7.3689(11) Å, c = 10.2011(13) Å, and β = 120.796(6)°. The structure was solved by using combined direct space methods and first-principles molecular dynamics simulated annealing. The Rietveld fit to the XRD pattern and the detailed structural information are shown in the Supporting Information, Figure S4, Tables S1 and S2. The fully relaxed structure from the first-principles calculations is illustrated in Figure 3.

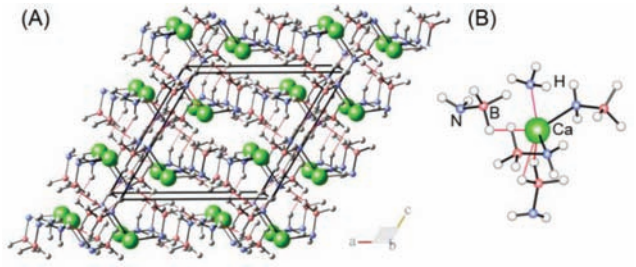

Figure 3. (A) Molecular packing and dihydrogen bonding network in the $Ca(NH_2BH_3)_2{\cdot}NH_3$ structure and (B) close contacts around the Ca^{2+} center. Calcium is represented by green spheres, nitrogen by blue spheres, boron by pink spheres, and hydrogen by white spheres. The red solid lines in (a) denote dihydrogen bonding while in (b) show the local coordination of Ca^{2+} with $H^{\delta-}$ (BH_3) and NH_3.

In $Ca(NH_2BH_3)_2{\cdot}NH_3$, the Ca^{2+} cation has a trigonal bipyramidal coordination geometry, surrounded by two N's of the $NH_2BH_3^-$ groups, two BH_3 of the $NH_2BH_3^-$ groups, and one NH_3 via electrostatic interactions and van der Waals interactions. The two Ca−N distances are 2.400 Å and 2.465 Å, close to the Ca−N bonds in $Ca(NH_2BH_3)_2$ (~2.466 Å)[11] and $Ca(NH_2BH_3)_2{\cdot}2NH_3$ (2.397−2.521 Å),[22] respectively, while the 2.472 Å Ca···NH_3 distance matches well with the adducted NH_3 observed in $Ca(NH_2BH_3)_2{\cdot}2NH_3$ (2.470 Å).[22] Ca···BH_3 interactions range between 2.669 Å and 3.182 Å, close to the Ca···B distances detected in $Ca(NH_2BH_3)_2$ and $Ca(NH_2BH_3)_2{\cdot}2NH_3$. The BH_3 acts as a versatile ligand, coordinating with Ca^{2+} via B−H···Ca^{2+} bond. As a result of the Ca−N interaction, the N−H bonds in the adducted NH_3 were lengthened (1.025 Å versus 1.020 Å in NH_3 gas). This is further evidenced by the absences of the high-frequency N−H stretching of NH_3 (~3444 cm^{-1}) in the FTIR spectra. A significant shortening of the B−N bond (1.535 and 1.558 Å versus 1.58 Å in AB[28−30]) and lengthening of the B−H bond (1.239 and 1.240 Å versus 1.18 Å in AB)[28−30] were also detected in $Ca(NH_2BH_3)_2{\cdot}NH_3$, revealing a strengthened B−N bond and weakened B−H bond, respectively, in the structure. These results agree with the observation of a substantial blue shift for B−N stretching in the FTIR spectra (Supporting Information, Figure S1) and a downfield shift of ^{11}B resonance of the postmilled sample (Figure 2). It is worthwhile to highlight the presence of the $H^{\delta-}\cdots H^{\delta+}$ dihydrogen bond network in the structure with bond distances ranging from 1.826 Å to 2.354 Å as another driving force for the structural stabilization. The shortest dihydrogen bond was identified to originate from the intermolecular interaction between coordinated NH_3 and the BH_3 of $NH_2BH_3^-$ of the adjacent molecule.

Figure 4 shows the neutron vibrational spectra of $Ca(NH_2BH_3)_2{\cdot}NH_3$. The observed phonon bands can be assigned

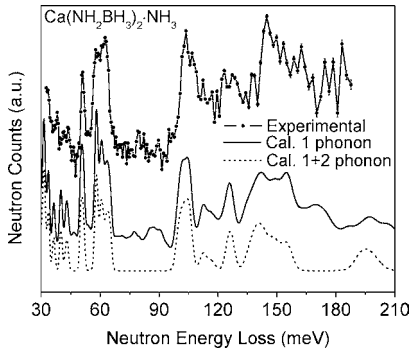

Figure 4. Observed and first-principles calculated neutron vibrational spectra of $Ca(NH_2BH_3)_2{\cdot}NH_3$ at 5 K. Error bars represent plus and minus the combined standard uncertainty.

to the librational modes (39−43 meV) of the NH_2BH_3 group, rotational modes of N−H (50−58 meV) in NH_2BH_3, librational modes of N−H in NH_3 (60−65 meV)), NH_2−BH_3 waggling and bending modes (99−105 meV), B−N stretching modes (112−117 meV), $NH_2BH_3^-$ deformation and torsion modes (125−127 meV; 135−137 meV), B−H and N−H bending modes in NH_2BH_3 (138−143 meV), bending modes of N−H in NH_3 (147−148 meV), scissoring modes of B−H (154−156 meV) and N−H (192−194 meV) in NH_2BH_3, and scissoring modes of N−H in NH_3 (198−200 meV). In general, the calculated spectra agree well with the observed neutron vibrational spectra, and thus further support the validity of the determined structure.

Hydrogen storage properties of $Ca(NH_2BH_3)_2{\cdot}NH_3$ were investigated under two conditions: open and closed systems. An open-system dehydrogenation was investigated by means of TPD-MS and TG-DSC. The TPD-MS measurement on $Ca(NH_2BH_3)_2{\cdot}NH_3$ (Figure 5) revealed a two-step decom-

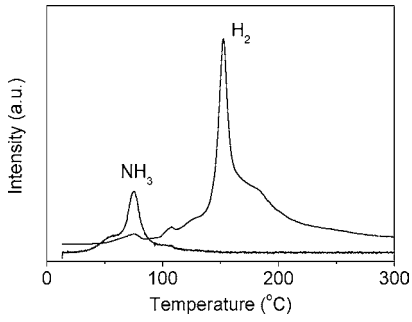

Figure 5. TPD-MS profiles of the postmilled $Ca(NH_2BH_3)_2{\cdot}NH_3$ sample with a ramping rate of 2 °C/min.

position with predominantly NH_3 gas released in the first step at temperatures <100 °C, while only H_2 is released in the second step in the temperature range of 100−300 °C, showing a great similarity with the decomposition of Ca-

dx.doi.org/10.1021/ic201898v | Inorg. Chem. 2012, 51, 1599−1603

$(NH_2BH_3)_2{\cdot}2NH_3$.[22] In comparison with the decomposition of $Mg(NH_2BH_3)_2{\cdot}NH_3$, the adducted NH_3 in $Ca(NH_2BH_3)_2{\cdot}NH_3$ is more weakly bound to the Ca^{2+}.[23] The TG-DSC results shown in Figure 6 also indicated an endothermic reaction in the

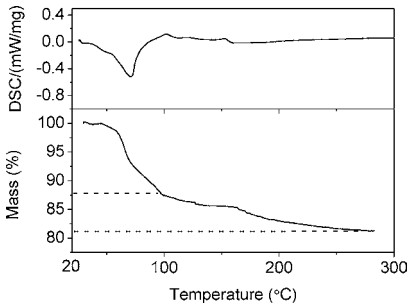

Figure 6. TG-DSC profiles of $Ca(NH_2BH_3)_2{\cdot}NH_3$ with a ramping rate of 2 °C/min.

first-step deammoniation process with a significant weight loss of 12.6 mass % [or 0.87 equivalents/formula unit of NH_3]. The second step (100−300 °C) is broad and results in a mass loss of 6.2%. This part of the mass loss may be attributed to the decomposition of calcium amidoborane that is formed after the deammoniation process. It is worthwhile to mention that the total mass loss for $Ca(NH_2BH_3)_2{\cdot}NH_3$ (18.8%) is less than the theoretical value for deammoniation (∼14.5%) and dehydrogenation (for $Ca(NH_2BH_3)_2$, ∼8 wt %), indicating that not all the NH_3 can be removed under TG-DSC measurement conditions. Instead, some may have been involved in the secondary reaction as evidenced by the concurrent release of H_2 at temperatures <100 °C.

However, when $Ca(NH_2BH_3)_2{\cdot}NH_3$ was heated in a closed-system, a different dehydrogenation behavior was detected. Volumetric release measurement on the $Ca(NH_2BH_3)_2{\cdot}NH_3$ sample revealed a two-step hydrogen release process with the first step occurring in the temperature range of ∼70−180 °C and the second step starting simultaneously right after the first step (see Figure 7). In the closed-system where NH_3 was

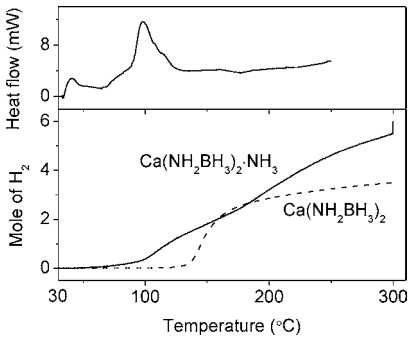

Figure 7. C80 DSC (top) and volumetric release (bottom) measurements on $Ca(NH_2BH_3)_2{\cdot}NH_3$ with a ramping rate of 0.5 °C/min. Volumetric release measurement on $Ca(NH_2BH_3)_2$ was included for comparison.

retained in the system as a result of its equilibrium pressure, NH_3 not only acts as an additional protic H source to react with amidoborane to release more H_2, but also promotes low-temperature dehydrogenation as consequences of the weakened B−H (amidoborane) and N−H (NH_3) bonds in the structure. A strong exothermic peak can be observed in the first dehydrogenation step, indicating a spontaneous H_2 release because of a reaction of NH_3 with BH_3 of the $NH_2BH_3^-$ group. The second dehydrogenation step, however, is a mild reaction. Upon dehydrogenation to 300 °C, a total release of 6 equiv. of H_2 (∼10.2 wt %) can be achieved, identical with that observed in $Mg(NH_2BH_3)_2{\cdot}NH_3$.[23] The NH_3 remaining in the gaseous product was quantified to be <0.1 equiv, indicating a more efficient NH_3 conversion to form H_2 than that observed in the decomposition of $Ca(NH_2BH_3)_2{\cdot}2NH_3$ in the closed-system heating process. The XRD pattern of the post-dehydrogenated sample demonstrates a broad signal for the amorphous phase (see Supporting Information, Figure S5). ^{11}B MAS NMR characterization (Figure 2) revealed the presence of a broad B−N resonance in the range of a 50−0 ppm chemical shift, agreeing with the observed broad B−N vibration at about 785 cm^{-1} (Supporting Information, Figure S1). In addition, no obvious B−H stretching in the sample was observed. Although the N−H stretching of the post dehydrogenated sample is also unapparent, the presence of broad N−H vibration[31] at about 1480 cm^{-1} suggested that the last H atom in the sample should be bound to nitrogen instead of boron. On the basis of the results described above, the following reaction is postulated:

$$Ca(NH_2BH_3)_2{\cdot}NH_3 \rightarrow CaB_2N_3H + 6H_2 \quad (3)$$

It is worth mentioning that a similar equation has been proposed for the decomposition of $Mg(NH_2BH_3)_2{\cdot}NH_3$, releasing 6 equiv. of H_2 and give rise to the formation of MgB_2N_3H (a Mg analogue).[12] Therefore, we deduce that the dehydrogenation of the ammoniate of the divalent (alkaline-earth) metal amidoborane would proceed via a similar dehydrogenation process.

CONCLUSION

In summary, we have demonstrated that the monoammoniate of calcium amidoborane can be synthesized by solid-state reaction between CaNH and AB. $Ca(NH_2BH_3)_2{\cdot}NH_3$ exhibits identical dehydrogenation properties with that of $Ca(NH_2BH_3)_2{\cdot}2NH_3$, that is, undergoing deammoniation at temperatures <100 °C in an open-system and giving rise to the formation of $Ca(NH_2BH_3)_2$. In a closed-system dehydrogenation, the presence of NH_3 in the structure promotes low-temperature dehydrogenation, releasing hydrogen at temperatures as low as 70 °C. A hydrogen-storage capacity of ∼10.2 wt % can be achieved upon heating to 300 °C with the detection of less than 0.1 equiv. of NH_3, showing higher hydrogen capacity with improved purity as compared to $Ca(NH_2BH_3)_2{\cdot}2NH_3$.

ASSOCIATED CONTENT

Supporting Information

FTIR and Raman spectra of $Ca(NH_2BH_3)_2{\cdot}NH_3$, $Ca(NH_2BH_3)_2{\cdot}2NH_3$, and AB, XRD patterns of the postmilled samples, Rietveld fit to the XRD pattern and crystallographic information file (CIF) of $Ca(NH_2BH_3)_2{\cdot}NH_3$, XRD pattern of the post dehydrogenated $Ca(NH_2BH_3)_2{\cdot}NH_3$, table of calculated structural parameter. This material is available free of charge via the Internet at http://pubs.acs.org.

AUTHOR INFORMATION

Corresponding Author

*E-mail: huiwu@nist.gov (H.W.), wgt@dicp.ac.cn (G.W.).

■ ACKNOWLEDGMENTS

This work was supported by National Program on Key Basic Research Project (973 project, No. 2010CB631304), the Hundred Talents Project and Knowledge Innovation Program of CAS (KJCX2-YW-H21), National Natural Science Foundation of China (No. 20971120, 10979051, and 20973162), the scholarship from the National University of Singapore, and was partially supported by U.S. DOE through EERE Grant DE-AI-01-05EE11104 (T.J.U.). The authors wish to thank BL14B1 of Shanghai Synchrotron Radiation Facility (SSRF) for providing the beam time.

■ REFERENCES

(1) Baitalow, F.; Baumann, J.; Wolf, G.; Jaenicke-Rossler, K.; Leitner, G. *Thermochim. Acta* **2002**, *391*, 159.
(2) Sit, V.; Geanangel, R. A.; Wendlandt, W. W. *Thermochim. Acta* **1987**, *113*, 379.
(3) Spielmann, J.; Bolte, M.; Harder, S. *Chem. Commun.* **2009**, 6934.
(4) Hill, M. S.; Kociok-Kohn, G.; Robinson, T. P. *Chem. Commun.* **2010**, *46*, 7587.
(5) Denney, M. C.; Pons, V.; Hebden, T. J.; Heinekey, D. M.; Goldberg, K. I. *J. Am. Chem. Soc.* **2006**, *128*, 12048.
(6) Jaska, C. A.; Temple, K.; Lough, A. J.; Manners, I. *J. Am. Chem. Soc.* **2003**, *125*, 9424.
(7) Xiong, Z. T.; Yong, C. K.; Wu, G. T.; Chen, P.; Shaw, W.; Karkamkar, A.; Autrey, T.; Jones, M. O.; Johnson, S. R.; Edwards, P. P.; David, W. I. F. *Nat. Mater.* **2008**, *7*, 138.
(8) Kang, X. D.; Fang, Z. Z.; Kong, L. Y.; Cheng, H. M.; Yao, X. D.; Lu, G. Q.; Wang, P. *Adv. Mater.* **2008**, *20*, 2756.
(9) Diyabalanage, H. V. K.; Nakagawa, T.; Shrestha, R. P.; Semelsberger, T. A.; Davis, B. L.; Scott, B. L.; Burrell, A. K.; David, W. I. F.; Ryan, K. R.; Jones, M. O.; Edwards, P. P. *J. Am. Chem. Soc.* **2010**, *132*, 11836.
(10) Diyabalanage, H. V. K.; Shrestha, R. P.; Semelsberger, T. A.; Scott, B. L.; Bowden, M. E.; Davis, B. L.; Burrell, A. K. *Angew. Chem., Int. Ed.* **2007**, *46*, 8995.
(11) Wu, H.; Zhou, W.; Yildirim, T. *J. Am. Chem. Soc.* **2008**, *130*, 14834.
(12) Zhang, Q. G.; Tang, C. X.; Fang, C. H.; Fang, F.; Sun, D.; Ouyang, L. Z.; Zhu, M. *J. Phys. Chem. C* **2010**, *114*, 1709.
(13) Genova, R. V.; Fijalkowski, K. J.; Budzianowski, A.; Grochala, W. *J. Alloys Compd.* **2010**, *499*, 144.
(14) Wu, H.; Zhou, W.; Pinkerton, F. E.; Meyer, M. S.; Yao, Q.; Gadipelli, S.; Udovic, T. J.; Yildirim, T.; Rush, J. J. *Chem. Commun.* **2011**, *47*, 4102.
(15) Kang, X.; Luo, J.; Zhang, Q.; Wang, P. *Dalton Trans.* **2011**, *40*, 3799.
(16) Fijalkowski, K. J.; Genova, R. V.; Filinchuk, Y.; Budzianowski, A.; Derzsi, M.; Jaroń, T.; Leszczyński, P. J.; Grochala, W. *Dalton Trans.* **2011**, *40*, 4407.
(17) Lee, T. B.; McKee, M. L. *Inorg. Chem.* **2009**, *48*, 7564.
(18) Kim, D. Y.; Singh, N. J.; Lee, H. M.; Kim, K. S. *Chem.—Eur. J.* **2009**, *15*, 5598.
(19) Kim, D. Y.; Lee, H. M.; Seo, J.; Shin, S. K.; Kim, K. S. *Phys. Chem. Chem. Phys.* **2010**, *12*, 5446.
(20) Luedtke, A. T.; Autrey, T. *Inorg. Chem.* **2010**, *49*, 3905.
(21) Spielmann, J.; Jansen, G.; Bandmann, H.; Harder, S. *Angew. Chem., Int. Ed.* **2008**, *47*, 6290.
(22) Chua, Y. S.; Wu, G. T.; Xiong, Z. T.; He, T.; Chen, P. *Chem. Mater.* **2009**, *21*, 4899.
(23) Chua, Y. S.; Wu, G. T.; Xiong, Z. T.; Karkamkar, A.; Guo, J. P.; Jian, M. X.; Wong, M. W.; Autrey, T.; Chen, P. *Chem. Commun.* **2010**, *46*, 5752.
(24) Graham, K. R.; Kemmitt, T.; Bowden, M. E. *Energy Environ. Sci.* **2009**, *2*, 706.
(25) Xia, G. L.; Yu, X. B.; Guo, Y. H.; Wu, Z.; Yang, C. Z.; Liu, H. K.; Dou, S. X. *Chem.—Eur. J.* **2010**, *16*, 3763.
(26) Xiong, Z. T.; Wu, G. T.; Hu, J. J.; Chen, P. *J. Alloys Compd.* **2007**, *441*, 152.
(27) Certain commercial suppliers are identified in this paper to foster understanding. Such identification does not imply recommendation or endorsement by the NIST.
(28) Hughes, E. W. *J. Am. Chem. Soc.* **1956**, *78*, 502.
(29) Hoon, C. F.; Reynhardt, E. C. *J. Phys. C: Solid State Phys.* **1983**, *16*, 6129.
(30) Klooster, W. T.; Koetzle, T. F.; Siegbahn, P. E. M.; Richardson, T. B.; Crabtree, R. H. *J. Am. Chem. Soc.* **1999**, *121*, 6337.
(31) Allis, D. G.; Kosmowski, M. E.; Hudson, B. S. *J. Am. Chem. Soc.* **2004**, *126*, 7756.